

Research Article

Evolution of Micron-Scale Pore Structure and Connectivity of Lignite during Pyrolysis

Qiaorong Meng¹,¹ Yangsheng Zhao,^{1,2} Zhiqin Kang,² Yong Wang,¹ Li Gao,¹
and Yongfeng Zhang¹

¹College of Mining Engineering, Taiyuan University of Technology, Taiyuan, Shanxi 030024, China

²Key Laboratory of In-situ Property-improving Mining of Ministry of Education, Taiyuan University of Technology, Taiyuan 030024, China

Correspondence should be addressed to Qiaorong Meng; 986168597@qq.com

Received 9 December 2019; Revised 5 March 2020; Accepted 19 March 2020; Published 10 April 2020

Academic Editor: Hom Kandel

Copyright © 2020 Qiaorong Meng et al. This is an open access article distributed under the Creative Commons Attribution License, which permits unrestricted use, distribution, and reproduction in any medium, provided the original work is properly cited.

Based on the high-precision microcomputed tomography (micro-CT) technology, the evolution of the μm -scale pore structure and connectivity of lignite during pyrolysis from room temperature to 600°C was studied. The results show that the pore connectivity of lignite increases with the increase of temperature, and the change of pore structure can be divided into four stages: the first stage is from room temperature to 100°C, characterized by generation and connection of small-diameter pores. The second stage is 100–200°C, characterized by rapid expansion and interconnection of pores due to the thermal cracking. The third stage is from 200°C to 450°C, characterized by the slow evolution of pore structure for pyrolysis. The fourth stage is from 450°C to 600°C, characterized by pore interconnection for pyrolysis. 200°C is the temperature at which the μm -scale pore structure of lignite changes dramatically. During the whole pyrolysis process from room temperature to 600°C, the pore quantity of lignite is mainly from the pores of a diameter of 0.65–3 μm . At 200°C and above, the pore volume of lignite is mainly from the pores with a diameter larger than 100 μm , but they are few. These research results have important theoretical reference values for the upgrading and pyrolysis of lignite.

1. Introduction

Lignite is the lowest grade coal, with low carbon content, high water content, easy weathering, easy spontaneous combustion, high volatile content, difficult storage and transportation, and serious air pollution during combustion. These characteristics limit the direct exploitation and utilization of lignite. However, lignite resources are abundant, and the world's lignite resources (2,622.9 billion tons) account for 24.4% of the world's total coal resources (107,539 million tons). The global energy shortage has reminded researchers of the economic value of lignite and its related processing technology. In recent years, significant research has focused on upgrading technologies for lignite to improve the quality of coal and obtain a more economical and safe utilization of lignite.

There are many lignite upgrading methods [1–3], but the basic technology can be divided into two processes: dehydration and pyrolysis. Nowadays, dehydration is a basic technology, while pyrolysis is a promising approach in the future. Coal pyrolysis is a process of transferring heat and mass. The coal itself is both the receptor of the pyrolysis and the carrier of the thermal mass during pyrolysis. The pores and cracks of coal act as the channels of heat and mass; in other words, the transmission of heat and gas depends on the pore structure during pyrolysis [4, 5]. Therefore, the evolution and connectivity of the pore structure directly influence the permeability of the coal seam and the gas production during pyrolysis.

There are many reports on the characteristics of pores and fractures of coal during pyrolysis. Many scholars have studied the pore structure characteristics of coal char under

high temperature and the factors affecting the pore structure of coal char, such as heating rate, moisture content, and volatile matter of parent coal [6–9]. These studies were based on coal char or pulverized coal, and the parameters of pore structure were detected by using adsorption methods and mercury intrusion porosimetry, which are mainly to detect the nanoscale pores and open pores. Nanoscale pores are mainly related to the adsorption and reserves of coalbed methane, while micron-scale pores, especially micron-scale open pores, play a key role in the migration of gas in coal, and their connectivity determines the permeability of coal. Luo et al. [10] used small-angle X-ray scattering (SAXS) to study open and closed pores; the grinding process of pulverized coal destroyed the micron-scale pore structure of coal and affected the accuracy of experimental results. Therefore, block samples of lignite are studied, and the pore structure of coal is observed by microcomputed tomography (micro-CT), which is a nondestructive testing technology.

Since the introduction of medical computer tomography (CT) in geological sciences, many applications have been worked out in rock component identification and rock structure damage [11]. Mathews et al. [12] reviewed the application of X-ray CT for the study of coal. Much of the initial work was to provide visualization of the internal complexity of coal, and then it allowed obtaining characteristics of pore and fracture structure, mineral composition, and deformation under different conditions [13, 14]. With the continuous development of X-ray CT technology, the resolution has developed from 100 μm to submicron, which makes it possible to research μm -sized pore and fracture in coal by CT. Liu et al. [15] characterized the mesopore pore connectivity of two high-rank coals by FIB-SEM and X-ray micro-CT. Yu et al. [16] investigated the micropore development of lean coal during pyrolysis by a new $\mu\text{225KvCT}$ system.

According to some basic experimental studies, it has been found that the calorific value of gas produced in lignite pyrolysis is high, reaching the calorific value of steam [17]. In order to avoid the environmental pollution and high cost of pyrolysis in the traditional high-temperature settling furnace, some scholars analyzed the in situ pyrolysis characteristics of lignite and clarified the feasibility of in situ pyrolysis for lignite [18, 19] and simulated the controllability of the pyrolysis working surface in the laboratory [20]. Therefore, the in situ pyrolysis of lignite is an economical and effective method of extraction to obtain oil and gas products. For many years, our research team has been committed to the related research of in situ heat injection mining of lignite. Niu et al. [21, 22] studied the change characteristics of the permeability and pore structure of lignite during in situ steam pyrolysis and found that the permeability and porosity increased with temperature. However, lignite is low-grade coal, and it is mainly composed of mesopores (0.1–1 μm) and macropores (greater than 1 μm), with the micropore and pore internal surface areas being relatively small [23], so the key factor to permeability is the μm -sized pores. In this study, the microfocus CT system was used to conduct CT and permeability tests on lignite samples to observe the variation process of the μm -

sized pore structure and analyze the development of pore connectivity during pyrolysis. This is a fundamental challenge in lignite upgrading by in situ pyrolysis.

2. Experimental System and Methodology

2.1. Microfocus CT Scanning System. A μ225Kv microfocus CT system is used to observe the internal structure. It is composed of an X-ray generator, turntable, the scanning detector, and a data reconstruction soft system. The schematic diagram of the CT scanning and analysis process is shown in Figure 1. The X-ray generator emits cone beam X-rays at the rock specimen placed on the turntable. After penetrating the specimen, the X-rays continue to transmit and are then received by the detector. The information obtained from the detector is recorded and rebuilt by the data processing center. The 2D and 3D structures of the specimen were formed and displayed by image processing.

The system can detect all kinds of metal and nonmetal materials without damage and can reconstruct 3D structural images with high spatial resolution. It can reflect the inner structure more comprehensively from multilayers and multiangles. The focus size of its X-ray source is less than 3 μm , and magnification is 400 times. It can detect pores with a diameter of 0.5 μm or cracks with a width of 1.0 μm . Therefore, it has been used widely to detect the microstructure of rocks with nondestructive testing.

2.2. Atmosphere Pyrolysis Furnace. To accurately obtain the evolution of the pores and fractures in the coal specimen at different temperatures, we designed a small portable atmosphere furnace with controllable temperature. The furnace was filled with argon gas when the specimen was heated. After the coal specimen is fixed on the CT machine, it is no longer disassembled when heated. The coal specimen was heated directly in the atmosphere furnace to a predetermined temperature and then scanned by CT, thereby ensuring that the specimen can be heated and scan in the same position and avoiding the scanning error caused by frequently clamping the specimen. The structure diagram of the atmosphere furnace is shown in Figure 2(a). The furnace is relatively small. It is cylinder shaped with a diameter of 100 mm and a height of 150 mm. It consists of four parts, including an iron shell, two insulating layers, and a chamber. Two insulating layers are shown in red profile lines in different directions, and the resistance wire is wound around the internal insulation layer. The chamber is 20 mm in diameter and 80 mm wide. A quartz rod is used to support the specimen, and a thermometer is put into the chamber. The atmosphere furnace is mounted on a support, and the support can move up and down so that the atmosphere furnace can be moved synchronously. When heating, we move the furnace and make the specimen mounted on the turntable in the chamber. The heating power is 300 W, and the temperature rises slowly to ensure accuracy with that of control precision is $\pm 1^\circ\text{C}$, and the filling gas is argon. The heating layout of the atmosphere furnace and the CT machine is shown in Figure 2(b).

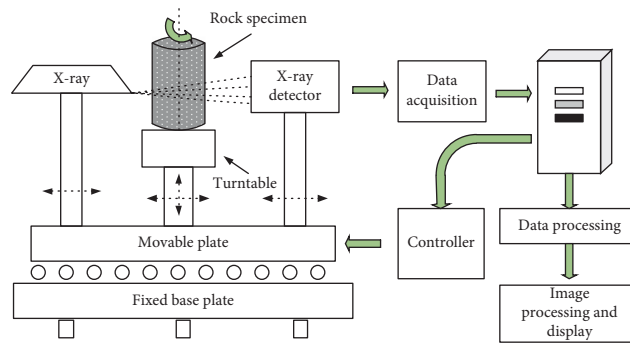


FIGURE 1: Schematic diagram of the $\mu 225\text{Kv}$ microfocus CT system for scanning and data processing.

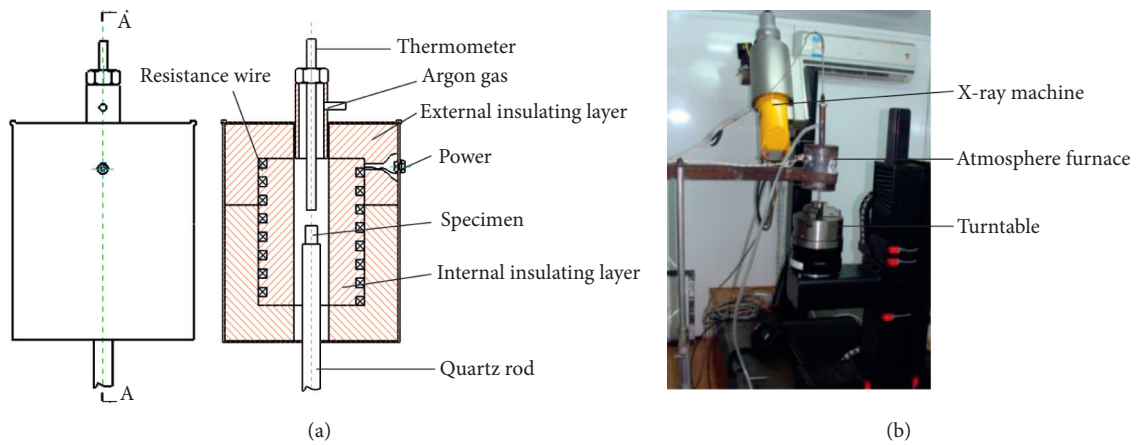


FIGURE 2: Experimental equipment. (a) Structure diagram of atmosphere furnace and (b) location of the CT machine and atmosphere furnace when heating.

2.3. *Specimen and Methodology.* The lignite sample was collected from Pingzhuang mine in the Chifeng city, Inner Mongolia, China. The coal quality indicators of air-dry basis are shown in Table 1. We made four nearly cylindrical coal specimens with 1 mm in diameter and 10 mm in height from the centers of different coal blocks, which can reduce the interference of external factors on the experimental data (such as weathering and drying).

First, the lignite specimen was supported by a quartz rod and clamped on the turntable, and a CT scan was performed at room temperature. The room temperature was about 20°C . After the CT scan was completed, the atmosphere furnace was moved onto the CT machine so that the specimen was in its chamber, and then the specimen was heated to 100°C and maintained for 30 mins and naturally cooled to room temperature, and then the atmosphere furnace was removed from the CT machine to perform a CT scan. Following the same fashion, with a temperature interval of 100°C , the lignite specimens were heated at a high temperature, cooled down, and then scanned by using the CT machine. The highest temperature tested in this research was 600°C , and the heating rate is $10^{\circ}\text{C}/\text{min}$. During the processes of heating, the lignite specimens were kept in an argon atmosphere to prevent oxidative combustion.

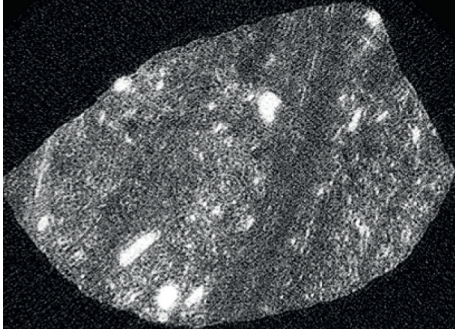
2.4. *Reconstruction of the 3D Digital Specimen.* After CT scanning, many section images of the scanned specimen were obtained, as shown in Figure 3. Every section image represents a $0.65\ \mu\text{m}$ thick layer of the specimen. The section images are in grayscale. The gray value represents the density of the scanned material, the white represents solid, and the blacks are pores. The brighter it is, the higher the density of the material is at the location.

All adjacent section images are superimposed to form a 3D digital coal sample, which can visually reflect pores and fractures in the coal specimen. A square of 731×731 (pixels, one pixel represents $0.65\ \mu\text{m}$) is selected on the section image of Figure 3, and then 100 successive layers are taken into a cube of $731 \times 731 \times 100$ voxels. The changes in the cube with increasing temperature are shown in Figure 4.

The pores of lignite are small at room temperature. When the temperature rises to 100°C , the pores become larger, but this change is not obvious. The most obvious change occurs at 200°C , many macropores of $50\ \mu\text{m}$ in diameter arise along the bedding direction. The pore morphology is diverse, and most of them are oval and slender rod-shaped. Every pore has obvious directionality. The direction of the larger diameter of pores is consistent with the direction of bedding, and the connectivity between the pores is poor. As the temperature continues to rise, the pore

TABLE 1: Coal quality indicators of lignite specimen.

Sample	Air dry moisture Mad (%)	Air dry ash Aad (%)	Air dry volatile Vad (%)	Air dry total sulfur St, ad (%)	Calorific value (MJ/kg)
Lignite	1.86	21	39.8	1.43	20.1

FIGURE 3: 2D section of the 556th slice of the lignite specimen at room temperature.

morphology gradually changes from ellipse to rod, and at 600°C, strip-like pores are predominant, and the original and new pores are interconnected.

3. Analysis of μm -Size Pore Structure Parameters of Lignite

Several $731 \times 731 \times 100$ digital cubes are selected in each coal specimen. Special CT scan image analysis software was used to obtain the data of the pore structure parameters from these cubes. All data are analyzed statistically. With an increase in temperature, lignite undergoes two processes: thermal cracking and pyrolysis, some small pores are generated, newly generated pores and existing pores are interconnected to form large pores, adjacent large pores are connected to form larger pores, these larger pores are irregular and like hollow clouds, and we call them pore clusters. The permeability of coal depends not only on porosity but also on the number, aperture, and volume of interconnected pore clusters.

3.1. Evolution Analysis of Porosity, Specific Surface Area, and Maximum Pore Cluster with Temperature. After being analyzed statistically, the pore structure parameters of lignite are presented in Table 2. Figures 5 and 6 are drawn based on the data given in Table 2. Figure 5 illustrates the relationship of porosity and the porosity of the max pore cluster with temperature, Figure 6 shows the relationship of total specific surface area and channel-specific surface area with temperature. As shown in Figures 5 and 6, the variation of pore structure parameters with temperature has been analyzed in four stages, i.e., the first stage (room temperature, -100°C), the second stage ($100\text{--}200^\circ\text{C}$), the third stage ($200\text{--}400^\circ\text{C}$), and the final stage ($400\text{--}600^\circ\text{C}$). The variation of pore structure parameters is the largest in the second stage, followed by the fourth stage, and the smallest and fluctuant in the third stage. The porosity of the maximum pore cluster

approaches the porosity gradually with increasing temperature, and the channel-specific surface area also approaches the total specific surface area, which indicates that the connectivity of lignite increases gradually with increasing temperature. From room temperature to 600°C , the porosity and the channel-specific surface area increase all the time, but the total specific surface area increases below 400°C and then decreases over 400°C , which indicates that the generation of newly formed pores and the interconnection of pores work equally well below 400°C , and over 400°C , the pore interconnection dominates.

In the first stage, when the temperature is below 100°C , the specific surface area increases more, and the porosity increases less, and the porosity of the maximum pore cluster is only 4.498% which indicates that there are many newly formed small pores in this stage, and most of them are closed pores. In the second stage, when the temperature ranges from 100°C to 200°C , the porosity of the maximum pore cluster and channel-specific surface area increase substantially by 23.3% and $0.2\text{ m}^2/\text{g}$, respectively. Pore structure changes dramatically, as shown in Figure 4, whereas the total specific surface area increases little. This indicates that some pores expand sharply and become larger in this stage, and some newly formed small pores are connected with existing pores to form larger ones, so the pore expansion is the main feature of this stage. In the third stage, when the temperature is from 200°C to 400°C , the specific surface area and channel-specific surface area increase slowly, while porosity and the porosity of max pore cluster first increase and then decrease, with a little fluctuation, and all of pore structure parameters change little, which indicates that this stage is a slow development process of pore generation and interconnection. At 400°C , the porosity is 31.075%; the porosity of the maximum pore cluster is 26.95% and is more than a quarter of the coal cube. According to the percolation theory, the coal rock without fracture has been completely permeated if its porosity is larger than 31% [24, 25]. Therefore, when the pyrolysis temperature reaches 400°C , the permeability of lignite changes from impermeability to complete penetration. In the fourth stage, when the temperature is from 400°C to 600°C , except for the total specific surface area reduction, other parameters increase rapidly, and the pores of lignite begin to expand rapidly for the second time. However, this expansion is different from the last one. In the second stage, the expansion of pore is mainly due to the thermal cracking caused by the different thermal stresses of gas-solid coupling during dehydration and degassing. While in the fourth stage, the pore dilatation originates mainly from the pyrolysis of coal organic matter. When the temperature exceeds 400°C , a large number of new pores are produced and connected with the original pores to form several larger pore clusters. Porous organic matter is

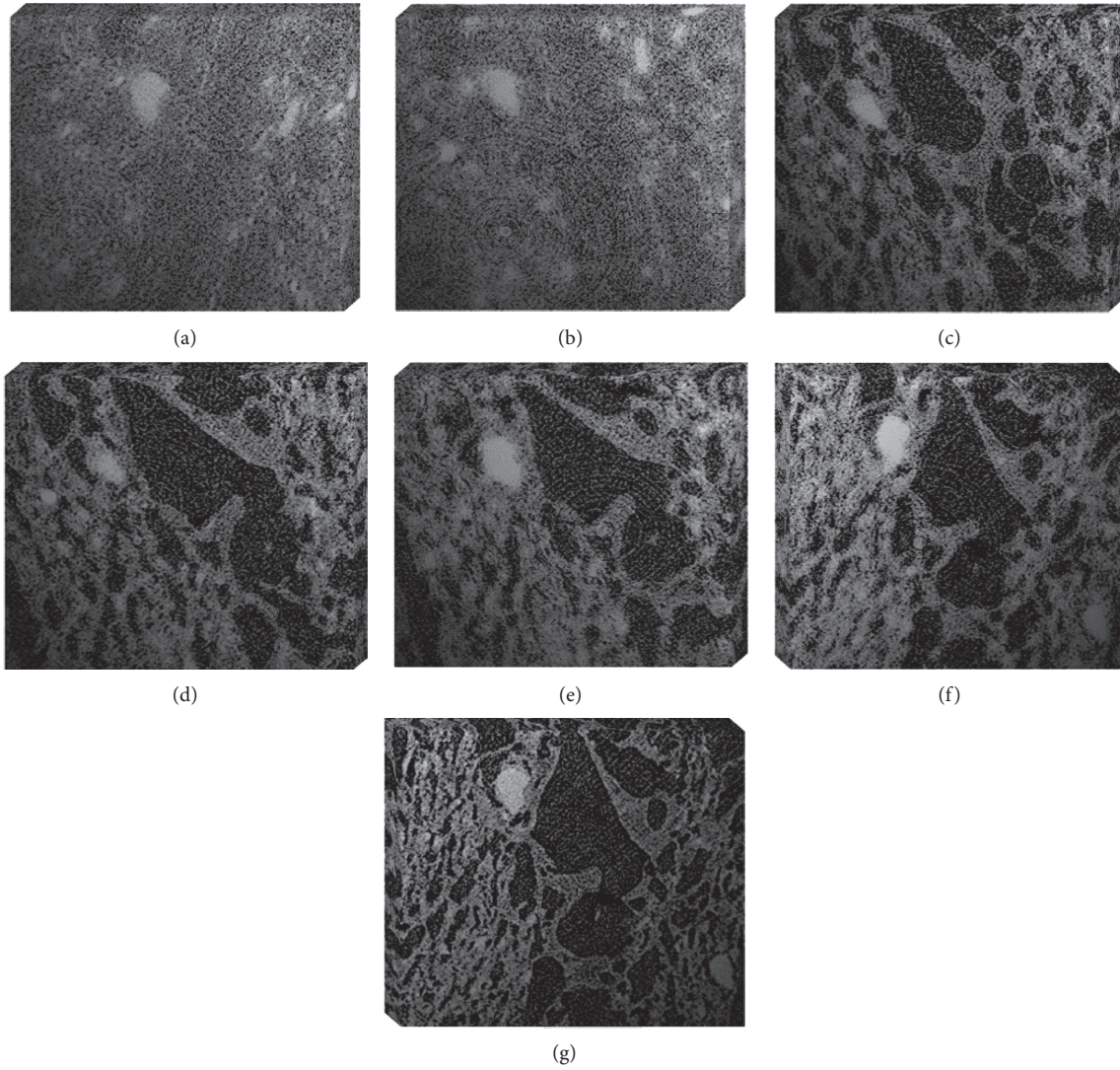


FIGURE 4: CT scan coal cube images of lignite at different temperature ($731 \times 731 \times 100$ voxels). (a) 20°C . (b) 100°C . (c) 200°C . (d) 300°C . (e) 400°C . (f) 500°C . (g) 600°C .

TABLE 2: Pore structural parameters of lignite at different temperature.

Temperature ($^\circ\text{C}$)	Porosity (%)	The porosity of max pore cluster (%)	Total specific surface area (m^2/g)	Channel-specific surface area (m^2/g)
20	8.988	0.76	0.281	0.020
100	12.37	4.498	0.363	0.116
200	29.983	27.85	0.374	0.316
300	30.343	28.40	0.375	0.318
400	27.73	26.95	0.376	0.321
500	29.75	27.828	0.355	0.327
600	36.53	35.405	0.346	0.320

depolymerized and disappears, forming larger pore, so total specific surface area decrease, but the permeability increases gradually.

3.2. The Distribution of Pores in Lignite with Temperature. Because the pore structure is irregular and pore cluster structure is more complex, it is difficult to make a statistical

analysis without a unified standard. So, each pore and pore cluster can be treated as a sphere of the same volume, where the sphere diameter is called the pore equivalent diameter, known as the diameter of the pore or pore cluster, and it is denoted by d :

$$d = \sqrt[3]{\frac{6nV_p}{\pi}}, \quad (1)$$

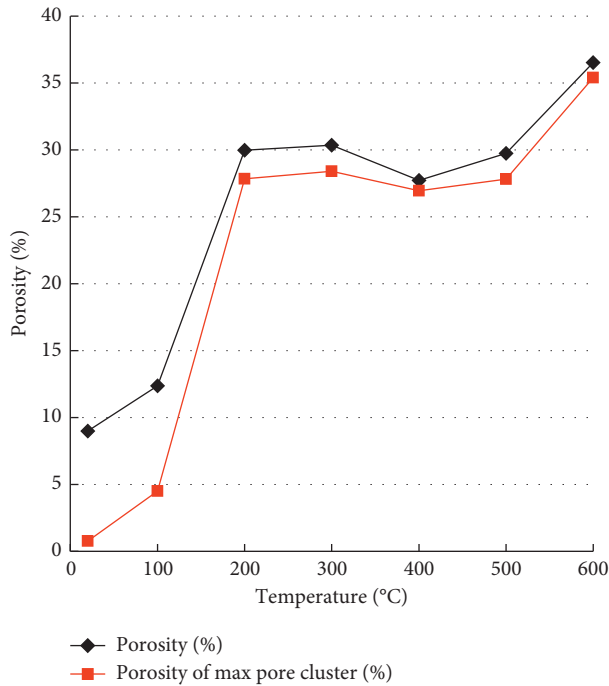


FIGURE 5: Porosity and the porosity of the maximum pore cluster at different temperatures.

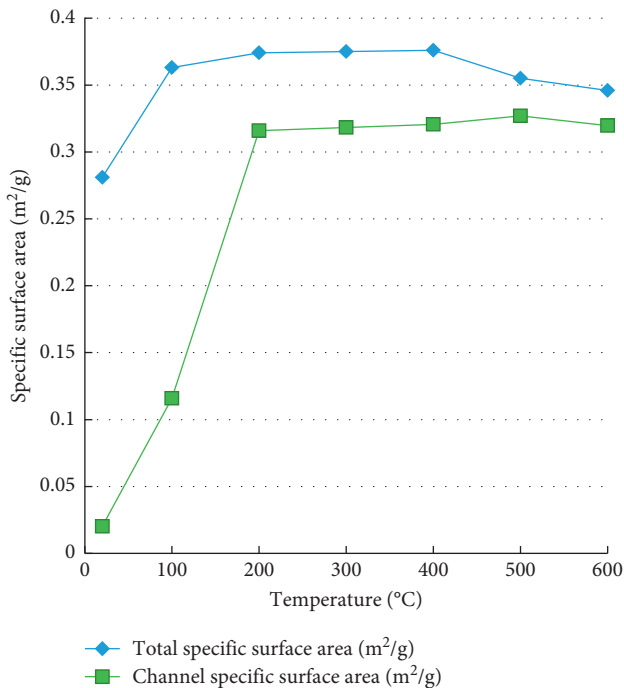


FIGURE 6: Specific surface area and channel-specific surface area under different temperatures.

where d is the equivalent pore diameter, n is the number of pixels in the pore or pore cluster, and V_p is the volume of one pixel, $0.65 \times 0.65 \times 0.65 \mu\text{m}^3$.

Figure 7 shows the variations in the proportion of μm -scale pores with pore diameter at different temperatures. The diameter of measurable pores ranges from 0.65 to 215.94 μm .

The proportion increases first and then decreases with increasing pore diameter. Thus, there is a maximum proportion of pores when the diameter is 1 μm at each temperature. The pores of 0.65–3 μm in diameter are dominant quantitatively, and their proportion gradually increases with the increase of temperature, which indicates that with increasing temperature, newly produced pores and existing pores interconnect and form larger pores, and pore number decreases (as shown Figure 8).

Figure 8 shows the variation of the number of pores with different diameters with the temperature. From Figure 8, it can be seen that the total number of pores and the numbers of pores with less than 100 μm diameter decrease with the increase of temperature and increase slightly at 400°C. The maximum reduction of the number is at 100–200°C, followed by 500–600°C. The number of pores with larger than 100 μm diameter is very small, 4 at 100°C, increased to 5 at 200°C, and remain 4 over 200°C, but their diameter becomes bigger and bigger with increasing temperature (as shown in Figure 7).

3.3. Characterization of Pore Volume in Lignite with Temperature. The volume of pore with different diameters and the maximum pore diameter under different temperatures are presented in Table 3. Figures 9 and 10 are drawn based on the data given in Table 3. From Fig. 9, it is evident that the total volume and the volume of pores with a larger than 100 μm diameter increase with temperature, and decrease slightly at 400°C. The maximum increase is at 100–200°C, followed by 500–600°C. When the temperature is higher than 200°C, the volume of pores with larger than 100 μm diameter accounts for the majority, and at 600°C, the volume proportion of pores with larger than 100 μm diameter reaches 97%. Both the volume of pores with the 0.65–3 μm diameter and the volume of pores with 3–100 μm diameter decrease with the increase of temperature, and when the temperature is higher than 200°C, they are very small; at 600°C, the proportion is 1.2% and 1.5%, respectively.

As can be seen from Figure 10, the maximum pore diameter increases with temperature and slightly decreases at 400°C. It almost triples from 78.093 μm at room temperature room to 215.943 μm at 600°C.

Considering the changes in pore volume and quantity with temperature, there is a noticeable phenomenon. At 200°C, the number of pores decreases sharply, but the volume increases sharply, and the maximum pore diameter has reached 201.901 μm and almost close to the maximum value of 215.943 μm . That is because a large number of newly produced and existing small pores interconnect to larger pore clusters with more than 100 μm diameter. So, at 200°C, the connectivity of the pores has been greatly improved. 200°C represents the temperature at which there is a dramatic change in the lignite pore structure.

3.4. Analysis of the Effect of Pyrolysis on the Pore Structure of Lignite. Lignite is low-rank coal, with high moisture content and volatile matter. Organic matter and inorganic matter in

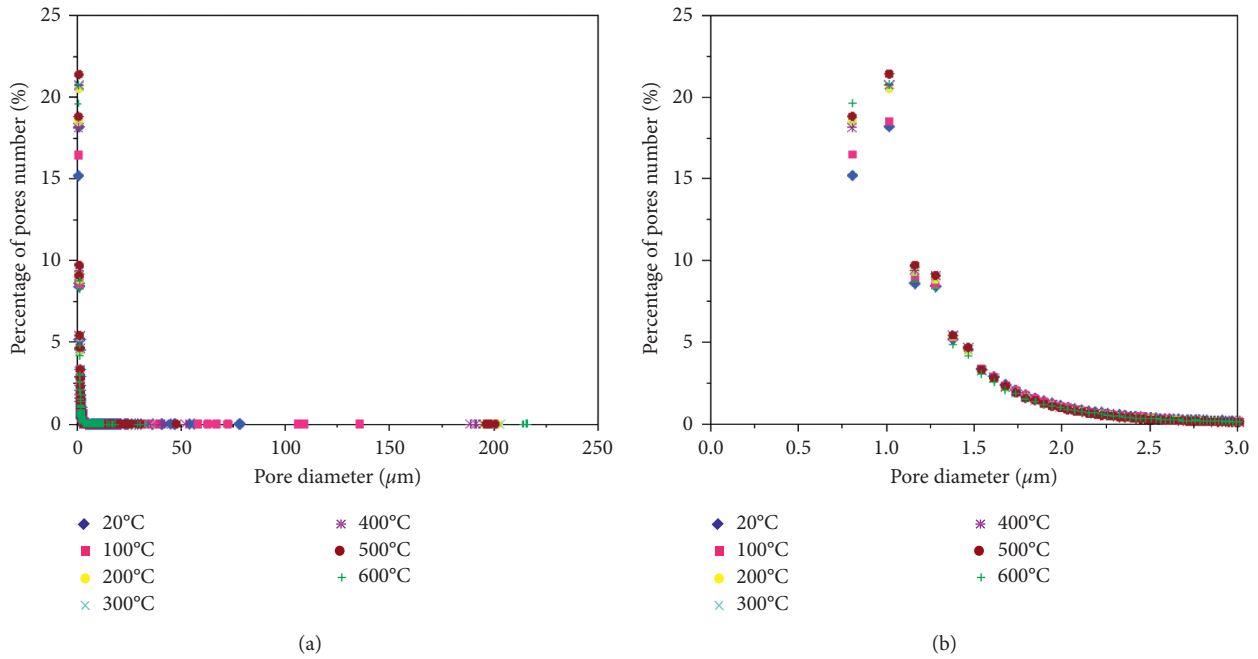


FIGURE 7: Pore distribution of lignite at different temperatures. (a) All measurable μm -sized pores; (b) 0.65–3 μm pores.

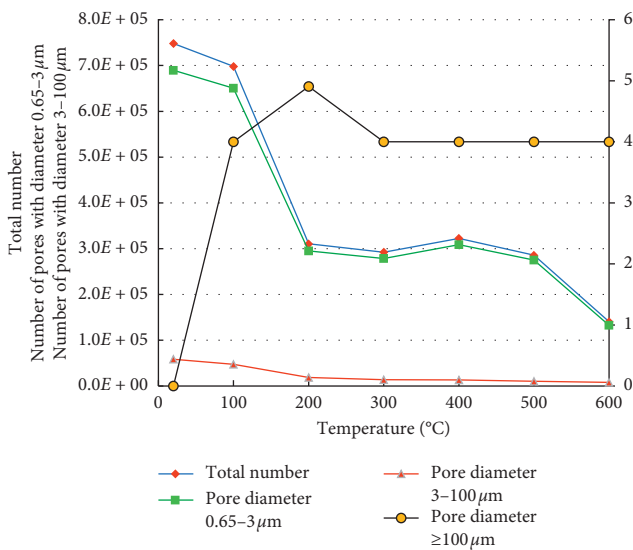


FIGURE 8: Variation in the number of pores with different diameters with the temperature.

coal undergo physical and chemical changes after heating, such as dehydration, degassing, depolymerization, and polycondensation. All of these physicochemical changes will directly affect the pore structure of the coal body.

When lignite samples are heated from room temperature to 200°C, the physical changes mainly occur. When the temperature is at 100°C, water in lignite evaporates gradually to form new pores. Water vapor thermal expands to enlarge the pores, and some of them interconnect to form larger pores when several thin pore walls break up. So, except for the number of pores, other pore structure parameters increase, and the pore diameter is mainly $0.65 \mu\text{m} < d \leq 3 \mu\text{m}$.

So, in this stage, the main feature is the generation and connection of small-diameter pores. When temperature increases from 100°C to 200°C, a lot of free and adsorbed gases undergo thermal expansion and make the pores of the original space larger. At the same time, coal particles also undergo thermal expansion. The interaction of these two kinds of thermal expansion causes the stress concentration on the pore wall, resulting in thermal cracking. So, a large number of pores interconnect to form larger pores, and larger pores connect into pore clusters. Porosity and specific surface area increase greatly, and the number and volume of pores with larger than 100 μm diameter increase greatly also, while the number and volume of pores with less than 100 μm diameter decrease. The maximum pore cluster becomes very big, and the pore connected channel increases. Therefore, the main characteristics are rapid expansion and interconnection of pores due to the thermal cracking from 100°C to 200°C, and 200°C is the temperature at which the pore structure of lignite changes most intensely.

When the temperature is from 200°C to 400°C, lignite is pyrolyzed, organic matter decomposes and depolymerizes to produce methane and carbon dioxide, and new pores are produced in the space of original organic matter. These newly produced gases are separated out of organic matter due to thermal expansion and newly produced pores connected with other pores around them. But, the thermal expansion of these gases has less pole in the expansion of pores volume because some of these gases can be freely released through the previously-formed channels. So, all of the pore parameters change slowly. When the temperature approaches 400°C, pyrolysis of coal matter produces less colloidal fragments and semicoke, and the fragments and semicoke fill and part the pores, which is the reason that the change of pore structure parameters fluctuates.

TABLE 3: Volume of pore and the maximum pore diameter.

Temperature (°C)	Total volume (μm^3)	Volume of pores with different diameter			Maximum pore diameter (μm)
		0.65–3 μm	3–100 μm	$\geq 100 \mu\text{m}$	
20	4639720	1522659	2599688	0	78.093
100	7261642	1367644	2037154	2639514	135.682
200	17598170	544172	583563	16347725	201.901
300	17811719	528424	512154	16668939	202.939
400	16274752	584657	508128	14710155	194.803
500	17462204	497099	391237	16335375	200.576
600	21329004	257305	316249	20782875	215.943

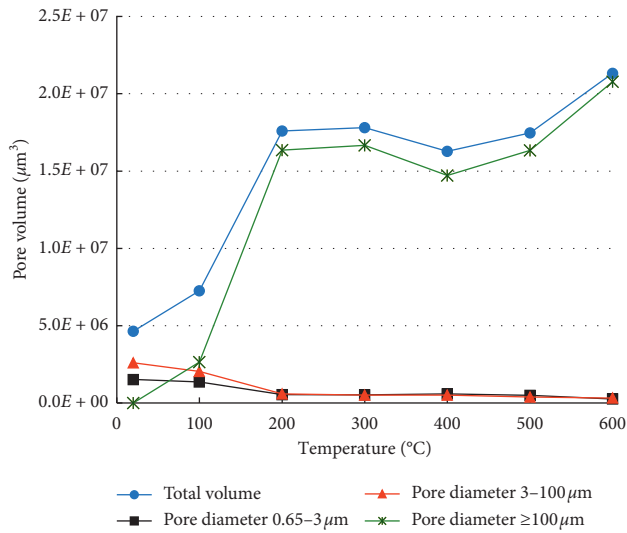


FIGURE 9: Variations in volume of pores with different diameters with temperature.

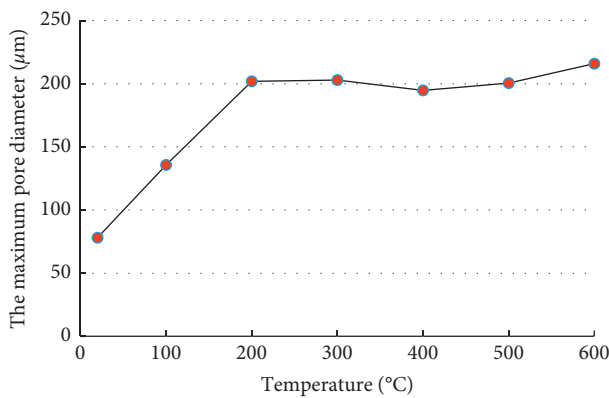


FIGURE 10: Variation in the maximum pore diameter with temperature.

When the temperature rises to 500°C, intense depolymerization reaction occurs in coal matter, and condensation reaction also occurs between liquid products and solid phases, and a large quantity of gases are produced, resulting in a large number of pores and microcracks, which makes pores interconnect and expand rapidly, so when the temperature is higher than 500°C, the second rapid change of pore structure of lignite begins. At 600°C, the porosity of the maximum pore cluster reaches 35.4%, and the ratio of the

channel-specific surface area reaches 92.37%, so the coal body achieves complete penetration.

From the abovementioned analysis, it can be seen that pyrolysis temperature has a significant influence on the pore structure. When the temperature is less than 200°C, the change of pore structure depends mainly on the thermal cracking, and when the temperature is higher than 200°C, it mainly depends on the pyrolysis products.

4. Discussion

From Figures 5, 6 and 8–10, it can be seen that each pore structure parameter of lignite fluctuates at 400°C, just opposite to the general trend of its change with the increase of temperature, so 400°C is a special temperature. At this temperature, the porosity and volume of the maximum pore cluster decrease, but the channel-specific surface area increases. Therefore, it is not straightforward to say that the connectivity becomes poor at 400°C, and this needs further study. Besides, it is worth noting that although the changing trend of pore structure parameters at 400–500°C is the same as that at 500–600°C, the slopes of the change curves are less than those of the latter. Based on the knowledge of lignite pyrolysis, lignite produces a large amount of semicoke and precipitate tar at about 450°C. Thus, the fluctuation of pore structure parameters should be about 450°C. Therefore, the third stage mentioned above should be changed from 200°C to 450°C, and the fourth stage should be from 450°C to 600°C.

5. Conclusions

The characteristics and development of μm -sized pore structure of lignite samples with diameter 1 mm were studied through micro-CT scan technology. The experiments were carried out at temperatures from room temperature to 600°C. Based on the systematical analysis of the experiment results, the following conclusions can be drawn:

- (1) When pyrolysis temperature increases from room temperature to 600°C, the evolution of pore structure of lignite can be divided into four stages. The first stage is from room temperature to 100°C, characterized by generation and connection of small-diameter pores and poor connectivity. The second stage is from 100 to 200°C, characterized by rapid expansion and interconnection of pores due to the thermal cracking. At 200°C, the pore structure of

lignite changes dramatically, and the connectivity is improved greatly. At 400°C, the coal sample achieved complete penetration. The third stage is from 200 to 450°C, marked by slow changes of pore structure with slow pyrolysis. The final stage is from 450 to 600°C, characterized by pores interconnection for pyrolysis. It is the second rapid change stage of the pore structure of lignite.

- (2) During the pyrolysis process from room temperature to 600°C, the μm -sized pores decrease in quantity and increase in volume. The number of pores with a diameter of 0.65–3 μm accounts for the vast majority, and the proportion gradually increases with increasing temperature. The volume of pores with a diameter larger than 100 μm accounts for the majority at 200°C and above and increases gradually with the increase of temperature.
- (3) During the pyrolysis process from room temperature to 600°C, the change of pore structure is caused by thermal cracking below 200°C and caused by pyrolysis above 200°C. The pore connectivity of lignite increases gradually with increasing temperature.

Data Availability

The data used to support the findings of Figures 5 and 6 are included within the article. The data used to support the findings of Figures 7–10 are included within the supplementary information file.

Conflicts of Interest

The authors declare that they have no conflicts of interest.

Acknowledgments

This research was financially supported by the National Natural Science Foundation of China (Grant no. 51974191). The authors thank the International Science Editing (<http://www.internationalscienceediting.com>) for editing this manuscript.

Supplementary Materials

This section includes the materials used to illustrate figures in this study. (*Supplementary Materials*)

References

- [1] S. Yuan, J. Liu, J. Wu et al., “Changes in the physicochemical characteristics and spontaneous combustion propensity of Ximeng lignite after hydrothermal dewatering,” *The Canadian Journal of Chemical Engineering*, vol. 96, no. 11, pp. 2387–2394, 2018.
- [2] Q. Zhou, T. Zou, M. Zhong et al., “Lignite upgrading by multi-stage fluidized bed pyrolysis,” *Fuel Processing Technology*, vol. 116, no. 12, pp. 35–43, 2013.
- [3] D. Li, C. Zhang, J. Xia, P. Tan, L. Yang, and G. Chen, “Evolution of organic sulfur in the thermal upgrading process of shengli lignite,” *Energy & Fuels*, vol. 27, no. 6, pp. 3446–3453, 2013.
- [4] Z. Yangsheng, Q. Fang, W. Zhijun, Z. Yuan, L. Weiguo, and M. Qiaorong, “Experimental investigation on correlation between permeability variation and pore structure during coal pyrolysis,” *Transport in Porous Media*, vol. 82, no. 2, pp. 401–412, 2010.
- [5] D.-W. Lee, J.-S. Bae, S.-J. Park, Y.-J. Lee, J.-C. Hong, and Y.-C. Choi, “The pore structure variation of coal char during pyrolysis and its relationship with char combustion reactivity,” *Industrial & Engineering Chemistry Research*, vol. 51, no. 42, pp. 13580–13588, 2012.
- [6] J. Zhou, H. Zhang, J. F. Lv, and G. X. Yue, “Effect of pyrolysis temperature on porous structure of anthracite chars produced at high temperature,” *Journal of Fuel Chemistry and Technology*, vol. 35, no. 2, pp. 155–159, 2007.
- [7] M. Wang, J. Zhang, S. Zhang et al., “Effect of pyrolysis conditions on the char surface area and pore distribution,” *Journal of China Coal Society*, vol. 33, no. 1, pp. 76–79, 2008.
- [8] Q. Chang, H. Li, T. Cui et al., “Effect of moisture content on gas release and pore structure development of wetted Shenfu coal during rapid pyrolysis,” *Journal of Fuel Chemistry and Technology*, vol. 45, no. 4, pp. 427–435, 2017.
- [9] Y. Chen, X. Wang, and He Rong, “Modeling changes of fractal pore structures in coal pyrolysis,” *Fuel*, vol. 90, no. 2, pp. 499–504, 2010.
- [10] L. Luo, J. Liu, Y. Zhang et al., “Application of small angle X-ray scattering in evaluation of pore structure of superfine pulverized coal/char,” *Fuel*, vol. 185, pp. 190–198, 2016.
- [11] M. Van Geet and R. Swennen, “Quantitative 3D-fracture analysis by means of microfocus X-Ray Computer Tomography (μCT): an example from coal,” *Geophysical Research Letters*, vol. 28, no. 17, pp. 3333–3336, 2001.
- [12] J. P. Mathews, Q. P. Campbell, H. Xu, and P. Halleck, “A review of the application of X-ray computed tomography to the study of coal,” *Fuel*, vol. 209, pp. 10–24, 2017.
- [13] Y. Yao, D. Liu, Y. Che, D. Tang, S. Tang, and W. Huang, “Non-destructive characterization of coal samples from China using microfocus X-ray computed tomography,” *International Journal of Coal Geology*, vol. 80, no. 2, pp. 113–123, 2009.
- [14] Z. Li, D. Liu, Y. Cai, P. G. Ranjith, and Y. Yao, “Multi-scale quantitative characterization of 3-D pore-fracture networks in bituminous and anthracite coals using FIB-SEM tomography and X-ray $\mu\text{-CT}$,” *Fuel*, vol. 209, pp. 43–53, 2017.
- [15] S. Liu, S. Sang, G. Wang et al., “FIB-SEM and X-ray CT characterization of interconnected pores in high-rank coal formed from regional metamorphism,” *Journal of Petroleum Science and Engineering*, vol. 148, pp. 21–31, 2017.
- [16] Y. Yu, W. Liang, Y. Hu, and Q. Meng, “Study of micro-pores development in lean coal with temperature,” *International Journal of Rock Mechanics and Mining Sciences*, vol. 51, no. 4, pp. 91–96, 2012.
- [17] Yi Wang, *Macroscopic and Microscopic Characteristics of High Temperature Steam Pyrolysis of Block Lignite*, Taiyuan University of Technology, Taiyuan, China, 2010.
- [18] H. Gao, Y. Zhu, T. Ma et al., “Thermal analysis on in-situ pyrolysis and kinetics characteristics of lignite,” *Journal of Nanjing Tech University (Natural Science Edition)*, vol. 34, no. 4, pp. 83–82, 2014.
- [19] H. Gao, Y. Zhu, F. Fu et al., “Pyrolysis of Hailar lignite in an autogenerated steam agent,” *Journal of Thermal Analysis and Calorimetry*, vol. 117, no. 2, pp. 973–978, 2014.

- [20] Z. Feng, *Theoretical and Experimental Study on In-Situ Steam Injection of Lignite for Oil and Gas Recovery*, Taiyuan University of Technology, Taiyuan, China, 2012.
- [21] S. Niu, Y. Zhao, and Y. Hu, "Experimental investigation of the temperature and pore pressure effect on permeability of lignite under the in-situ condition," *Transport in Porous Media*, vol. 101, no. 1, pp. 137–148, 2014.
- [22] S. Niu, *Experimental Investigation of the High-Temperature Permeability and Microscope Characteristic of Lignite and Numerical Simulation of the In-Situ-Oil-Gas Exploitation of Lignite by Steam Injection*, Taiyuan University of Technology, Taiyuan, China, 2012.
- [23] X. Zhang, B. Han, J. Li et al., "CBM storage character of lignite and gas content estimate method," *Coal Geology & Exploration*, vol. 34, no. 3, pp. 28–31, 2006.
- [24] A. H. Thompson, A. J. Katz, and C. E. Krohn, "The microgeometry and transport properties of sedimentary rock," *Advances in Physics*, vol. 36, no. 5, pp. 625–694, 1987.
- [25] Z. Feng, Y. Zhao, and Z. Wen, "Percolation mechanism of fractured coal rocks as dual-continua," *Chinese Journal of Rock Mechanics and Engineering*, vol. 25, no. 2, pp. 236–240, 2005.